 doi:10.20944/preprints201809.0569.v1

Chemotherapeutic Drug Functionalized Nanoparticles are Beneficial When Treating Breast Cancer Via Magnetic Hyperthermia

Susann Piehler[1], Heidi Dähring[1], Julia Grandke[1], Julia Göring[1]; Pierre Couleaud[2,3]; Antonio Aires[2,3], Aitziber L. Cortajarena[2,3,+]; José Courty[4]; Alfonso Latorre[2,3]; Álvaro Somoza[2,3]; Rodolfo Miranda[2,3]; Ingrid Hilger [1]

[1]Institute for Diagnostic and Interventional Radiology, Jena University Hospital – Friedrich Schiller University Jena, D-07740 Jena, Germany, susann.piehler@med.uni-jena.de; dheidi@t-online.de; julia.grandke@gmail.com ; julia.goering@med.uni-jena.de; ingrid.hilger@med.uni-jena.de

[2]Instituto Madrileño de Estudios Avanzados en Nanociencia (IMDEA Nanociencia), Campus Universitario de Cantoblanco, 28049 Madrid, Spain; emails: couleaud.pierre@gmail.com; antonio.aires@imdea.org; aitziber.lopezcortajarena@imdea.org; alfonso.latorre@imdea.org; alvaro.somoza@imdea.org; rodolfo.miranda@imdea.org

[3]Unidad Asociada de Nanobiotecnología CNB-CSIC & IMDEA Nanociencia, Campus Universitario de Cantoblanco, 28049 Madrid, Spain

[4]Laboratoire CRRET, Université Paris EST Créteil, 61 Avenue du Général de Gaulle, 94010 Créteil, France, email: courty@u-pec.fr

Corresponding author: Prof. Dr. Ingrid Hilger, Institute for Diagnostic and Interventional Radiology, University Hospital Jena, Research Center Lobeda, Am Klinikum 1 D-07747 Jena, Germany. Phone: 0049-3641-9325921, Fax: 0049-3641-9325922, e-mail: ingrid.hilger@med.uni-jena.demailto:

Preprints (www.preprints.org) | NOT PEER-REVIEWED | Posted: 28 September 2018 doi:10.20944/preprints201809.0569.v1

Abstract

Doxorubicin (DOX) is a frequently used chemotherapeutic drug for breast cancer, but its site specificity and local internalization into tumor cells is rather low. In this paper we conjugated magnetic nanoparticles (MNPs) with DOX and/or a pseudopeptide NucAnt (N6L) as modality to enhance DOX-induced antitumor effects in breast cancer cells (BT474). In this context, we determined cellular uptake of MNP formulations, analyzed cell viability and expression of apoptotic and cell cycle proteins after magnetic hyperthermia (43°C, 1 h) *in vivo* and *in vitro*. We have shown that i) the presence of N6L on the surface of DOX-functionalized MNPs increases their internalization into a target cells and potentiates the cytotoxic potential of the anticancer drug, ii) in combination with hyperthermia, DOX functionalized MNPs influence the expression of apoptotic and cell cycle proteins, and also favors tumor regression in vivo. Our data show that intratumoral application of DOX coupled MNPs is able to overcome biological barriers to chemotherapeutic drugs, enabling them to penetrate into the target cells. Combined with hyperthermia these MNPs can be an effective method in enhancing the localised delivery and penetration of DOX into breast cancer cells.

Key words: magnetic hyperthermia, magnetic nanoparticles (MNP), doxorubicin (DOX), NucAnt (N6L), breast cancer, mouse model

Preprints (www.preprints.org) | NOT PEER-REVIEWED | Posted: 28 September 2018 doi:10.20944/preprints201809.0569.v1

1 Introduction

Chemotherapeutic drugs play an important role in cancer treatment. Most of them show complex mechanisms of action. One example is the drug Doxorubicin (DOX), an anthracycline antibiotic, which intercalates with DNA , interrupts topoisomerase II activity and induces free radicals resulting in oxidative damage and DNA double-strand breaks [1], [2], [3], [4], [5]. In turn, DNA damage inhibits cell proliferation and activates cell cycle arrest or leads to apoptosis [6], [7]. Moreover DOX is the most potent and frequently used chemotherapeutic drug for various malignancies, including cancer of the breast, lung and aggressive lymphomas [8], [4]. However, DOX is not only cytotoxic to rapidly proliferating cancer cells but also damages healthy normal tissue and cells to a considerable extent. This is responsible for toxic side effects including myelosuppression, mucositis, stomatitis, alopecia and serious complications such as cardiotoxicity and hepatotoxicity [9], [10], [8]. Therefore it is difficult to achieve an adequate chemotherapeutic dosage at the target region through systemic application and the clinical use of the drug is limited. To overcome the problem, there are various approaches attempting to reduce toxicity of DOX while the drug delivery to target tissue and efficacy should be retained or improved at best. One strategy is the use of nanomedicine or nanotherapeutic delivery systems, which provide the possibility to selectively accumulate DOX at target tissue after selective conjugation [11]. Another promising approach is the functionalization of iron oxide magnetic nanoparticles (MNP) with DOX and their utilization in combination with hyperthermia. In general, MNPs release heat during exposure to an alternating magnetic field (AMF) of appropriate amplitude and frequency and this results in so-called magnetic hyperthermia.

In the last years, there are several preclinical approaches indicating an efficient treatment of various cancer cells with DOX-functionalized iron oxide nanoparticles in combination with hyperthermia, including a ovarian carcinoma cell line, a murine melanoma model, in vitro and in vivo therapy of rat glioma or breast cancer cell line [12], [13], [14], [15]. But nevertheless the studies known so far lack a corresponding statement according to the benefits over the conventional therapy [16]. It is very plausible that there are differences in pharmacokinetics

Preprints (www.preprints.org) | NOT PEER-REVIEWED | Posted: 28 September 2018 doi:10.20944/preprints201809.0569.v1

between the free anticancer drug DOX, DOX-functionalized MNPs and MNPs alone in vivo as well as in vitro that have to be evaluated. It is still unclear to which extent the presence of DOX really induces an additive effect to hyperthermia from a pathobiological view. Moreover last recent research activities aimed towards enhanced site specificity and internalization of drug carriers in general and of DOX-functionalized MNPs into tumor cells in particular, with the help of multifunctional nanoparticles [17], [18]. The development currently remains a challenge.

Furthermore it is known that the therapeutic outcome of hyperthermia depends on target-oriented application of thermal stress [19]. Here, the internalization of magnetic nanoparticles into cancer cells bears high potential to improve magnetic hyperthermia therapy [19]. In this context, the multivalent pseudopeptide NuCant (N6L) is of particular interest. The synthetic peptide binds to nucleolin, a nucleoprotein, which is selectively overexpressed on cell surface in various tumor cells [20], [21]. After binding, cell-surface nucleolin is able to shuttle N6L to the nucleus, where it mediates its lethal effects. N6L exhibits anti-tumor activities by inhibiting tumor growth, and furthermore it is a proapoptodic molecule and inhibits angiogenesis [21]. Nevertheless, so far it is not known if N6L could potentiate the effect of MNPs functionalized with DOX.

In the present study we search for modalities that can enhance DOX-induced antitumor effects in breast cancer cells and therefore we investigate if: i) the presence of N6L on the surface of MNPs functionalized with DOX increases the internalization into a breast cancer cell line and potentiates the cytotoxic potential of the anticancer drug, ii) the treatment of target cells with DOX functionalized MNPs combined with hyperthermia influences the expression of apoptodic proteins as well as proteins related to the cell cycle, iii) DOX functionalized MNPs in combination with hyperthermia favor tumor regression in vivo and if the in vivo treatment exhibits comparable expression pattern of apoptodic and cell cycle proteins with the in vitro situation.

2 Results

Preprints (www.preprints.org) | NOT PEER-REVIEWED | Posted: 28 September 2018 doi:10.20944/preprints201809.0569.v1

2.1 MF66-MNP formulations show a good heating potential and the presence of N6L on surface of MNPs conjugated with DOX augments internalization. All MNPs exhibited an iron oxide core diameter of approximately 12 nm (table 1). In general, the conjugation of MF66 increased their hydrodynamic diameter, whereby the bi-conjugated MF66-N6LDOX-MNPs showed the largest increase in size (table 1). The zeta potential decreased upon functionalization (table 1). As expected, the investigated MNP formulations displayed highest ILP values as suspension in water and a reduction upon increasing degree of immobilization (10% polyvinyl alcohol and cells) of MNPs (figure 1A). The strongest ILP reduction occurred during immobilization of MNPs conjugated with DOX and additionally N6L in BT474 cells but these MNPs still exhibited a good heating potential (figure 1A). All MNP formulations were internalized successfully by BT474 cells but with different extents. The bi-conjugated MF66-N6LDOX-MNP showed the best cellular uptake concluding that the presence of N6L on the DOX functionalized MNPs enhanced the internalization (figure 1B). Moreover, the internalization and cellular uptake was examined by optical microscopy and revealed comparable results (suppl. figure 2).

Table 1: Characterization of non-/ functionalized MF66-MNPs.

	MF66	MF66-DOX	MF66-N6L	MF66-N6LDOX
Core size [nm]	11.7	11.7	11.7	11.7
Coating	DMSA	DMSA	DMSA	DMSA
Functionalization [per g Fe]	none	40 µmol DOX	3.5 µmol N6L	40 µmol DOX 3.5 µmol N6L
Hydrodynamic diameter [nm]	89 ± 0.5	116 ± 0.6	115 ± 0.6	143 ± 3.8
PDI	0.36	0.39	0.23	0.29
Zeta potential [mV]	-46 ± 0.7	-37 ± 0.3	-40 ± 0.6	-33 ± 0.8

Preprints (www.preprints.org) | NOT PEER-REVIEWED | Posted: 28 September 2018 doi:10.20944/preprints201809.0569.v1

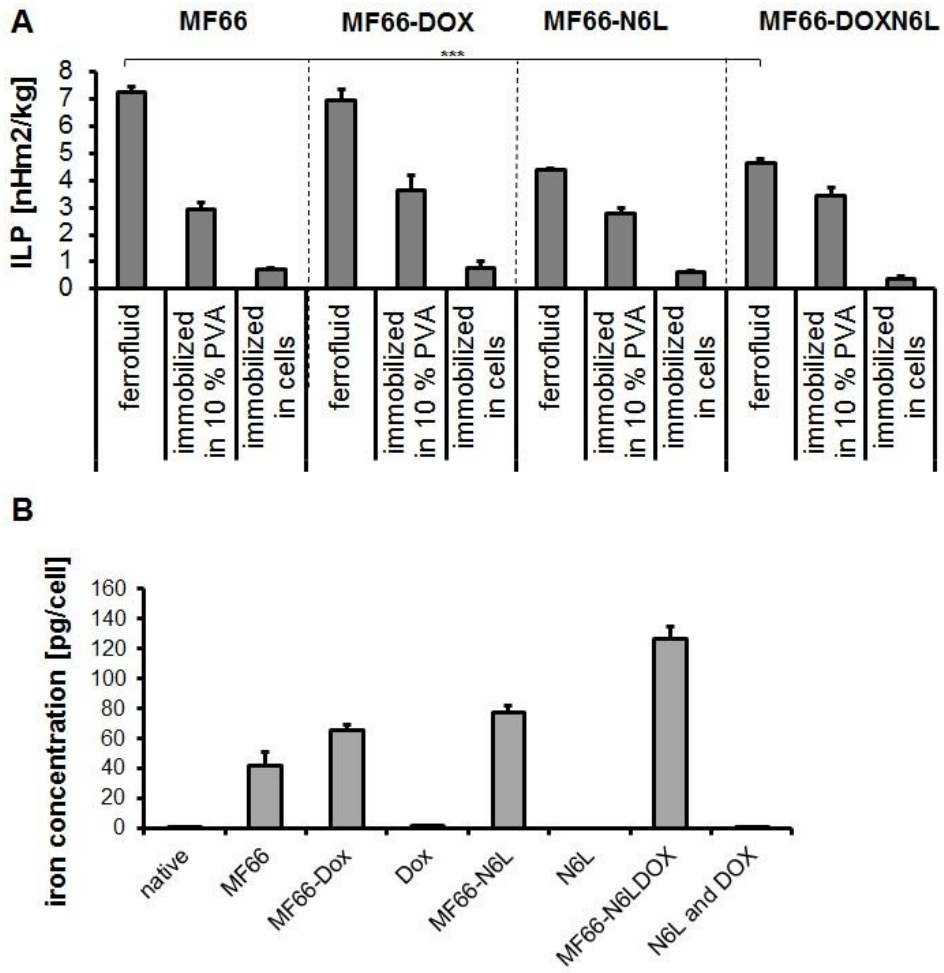

Figure 1. Characterization of heating potential and their cellular uptake in vitro. A) ILP values of MNPs suspended in water, immobilized in 10% polyvinyl alcohol (PVA) as well as in cells. B) Intracellular iron content measured in BT474 cells at 24 h after incubation with MNP formulations. Means of SEM of n ≥ 6 samples/group.

2.2 In combination with hyperthermia, functionalized N6L potentiates the cytotoxic effect of DOX functionalized MNPs on BT474 cells. According to the application modalities of DOX (free agent alone, in combination with N6L functionalized MNPs or additionally with hyperthermia) there is a gradual increase of the cytotoxic potential on BT474 cells. In this context the most prominent cytotoxic effect was observed when DOX conjugated MNPs were combined with magnetic hyperthermia with increasing incubation time after hyperthermia treatment compared to application of DOX conjugated MNPs alone and the free ligand (figure

Preprints (www.preprints.org) | NOT PEER-REVIEWED | Posted: 28 September 2018 doi:10.20944/preprints201809.0569.v1

2A-C). Furthermore the functionalization of MNPs with DOX and additionally N6L even exerts a stronger inhibition of BT474 cell growth than conjugation with DOX alone after hyperthermia treatment. Therefore N6L strengthened the cytotoxic effect of DOX functionalized MNPs in BT474 cells.

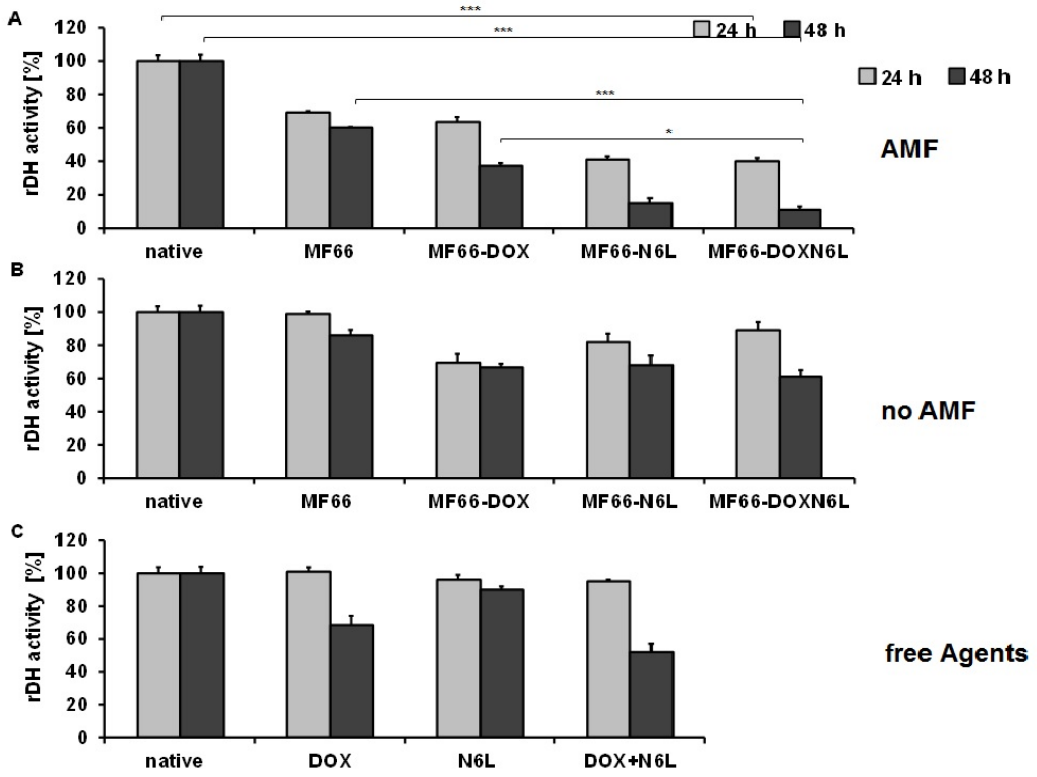

Figure 2. Magnetic hyperthermia with functionalized MNPs leads to growth inhibition of BT474 cells. The relative dehydrogenase activity was measured 24 h or 48 h after incubation **A)** with MNP formulations and AMF treatment, **B)** MNP application without AMF and **C)** treatment or the free ligands. AMF settings: H=23.9 kA m−1, f=410 kHz, 43 °C for 60 min. Means and SEM of three individual experiments with three parallels each.

To confirm the cytotoxic effect of magnetic hyperthermia and DOX conjugated MNP on BT474 cells morphologically, microscopic analyses were performed. These analyses clearly revealed morphological changes and detachment of BT474 cells after combined treatment of magnetic hyperthermia and functionalized MNPs most pronounced 48 h after treatment (figure 3). Here, the majority of cells showed rounded phenotypes after combined treatment of bi-functionalized MNPs (DOX and N6L) and magnetic hyperthermia (figure 3).

Preprints (www.preprints.org) | NOT PEER-REVIEWED | Posted: 28 September 2018 doi:10.20944/preprints201809.0569.v1

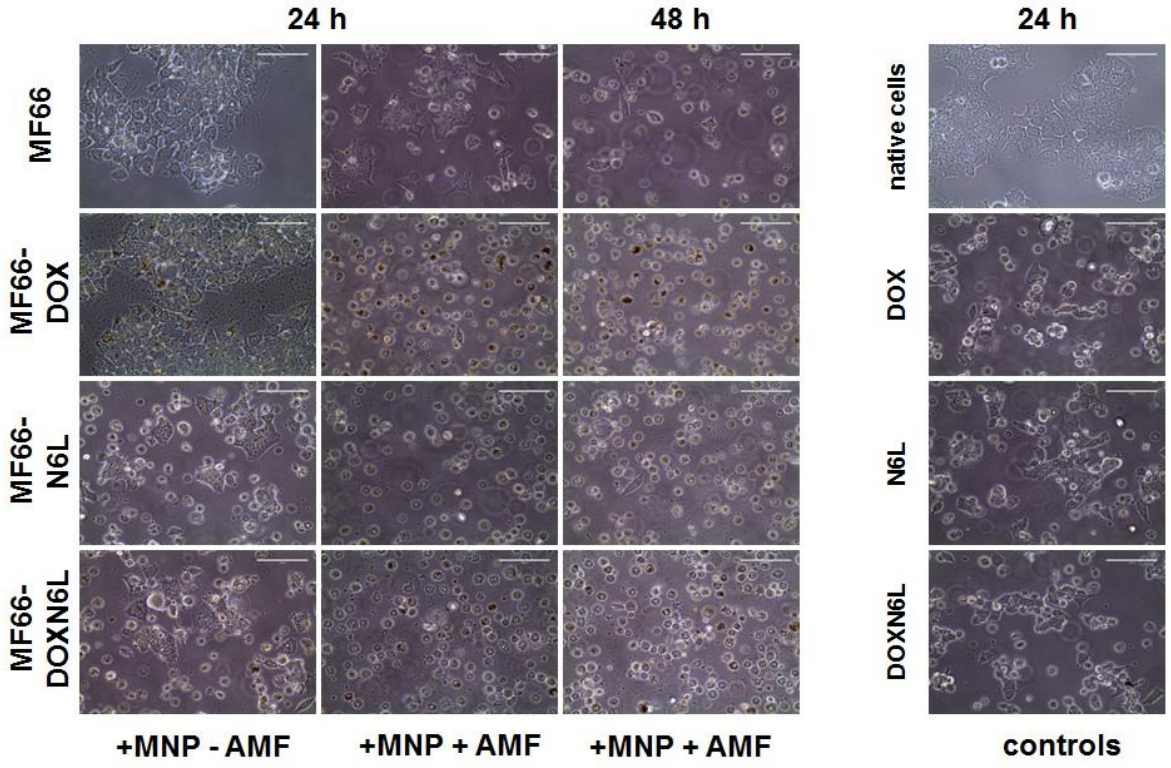

Figure 3. Magnetic hyperthermia in combination with MNP formulations induced morphological changes and detachment of BT474 cells. Representative macroscopic images of BT474 cells, incubated with the different MF66 formulations (100 µg Fe/ml, 24h), 24 h or 48 h post magnetic hyperthermia (+MNP/+AMF), MNP control (+MNP/-AMF), free agent controls (DOX, N6L or both) as well as untreated controls (native BT474). Scale bar = 100 µm.

2.3 The free ligand DOX induces cell death and the combination of magnetic hyperthermia and DOX functionalized MNPs arrested BT474 cells in the G2/M phase of the cell cycle. BT474 cells exposed to DOX and DOX-N6L conjugated MNPs in presence of magnetic hyperthermia remarkably downregulated pro-apoptodic markers p53, caspase3 and PARP compared to cells treated with free agent DOX and DOX-MNPs in absence of hyperthermia (24 h and 48 h post magnetic hyperthermia, figure 4A, B). Interestingly, the absence of magnetic hyperthermia fostered the expression of p53 and caspase 3 in cells treated with DOX functionalized MNPs as well as DOX and N6L conjugated MNPs with

Preprints (www.preprints.org) | NOT PEER-REVIEWED | Posted: 28 September 2018 doi:10.20944/preprints201809.0569.v1

increasing time after treatment (48 h post hyperthermia), whereas the accumulation of PARP was not detectable at all (figure 4B). The most pronounced activation of the mentioned apoptotic proteins was visible in cells treated with the free ligand DOX and with DOX and N6L (figure 4A, B). Only the free drugs led to an increased expression of PARP in treated cells. Furthermore the analysis of expression of cell cycle proteins revealed an up-regulation of CHK2 and cyclin B1 in BT474 cells treated with the free ligand DOX or a combination of DOX and N6L most prominent 24 h and to lesser extent 48 h after treatment, indicating an arrest of the cells in the G1/S phase and G2/M phase, respectively (figure 4A, B). Interestingly, at a later time after treatment (48 h) DOX functionalized MNPs in combination with magnetic hyperthermia exhibited a considerable induction of expression of PLK1 and to lesser extent of cyclin B1 and thereby arresting BT474 cells in the G2/M phase (figure 4B). However, this effect was not observable when cells exposed to the bi-functionalized (DOX and N6L) MNPs in presence of magnetic hyperthermia but it was detectable in absence of them (figure 4B).

Preprints (www.preprints.org) | NOT PEER-REVIEWED | Posted: 28 September 2018 doi:10.20944/preprints201809.0569.v1

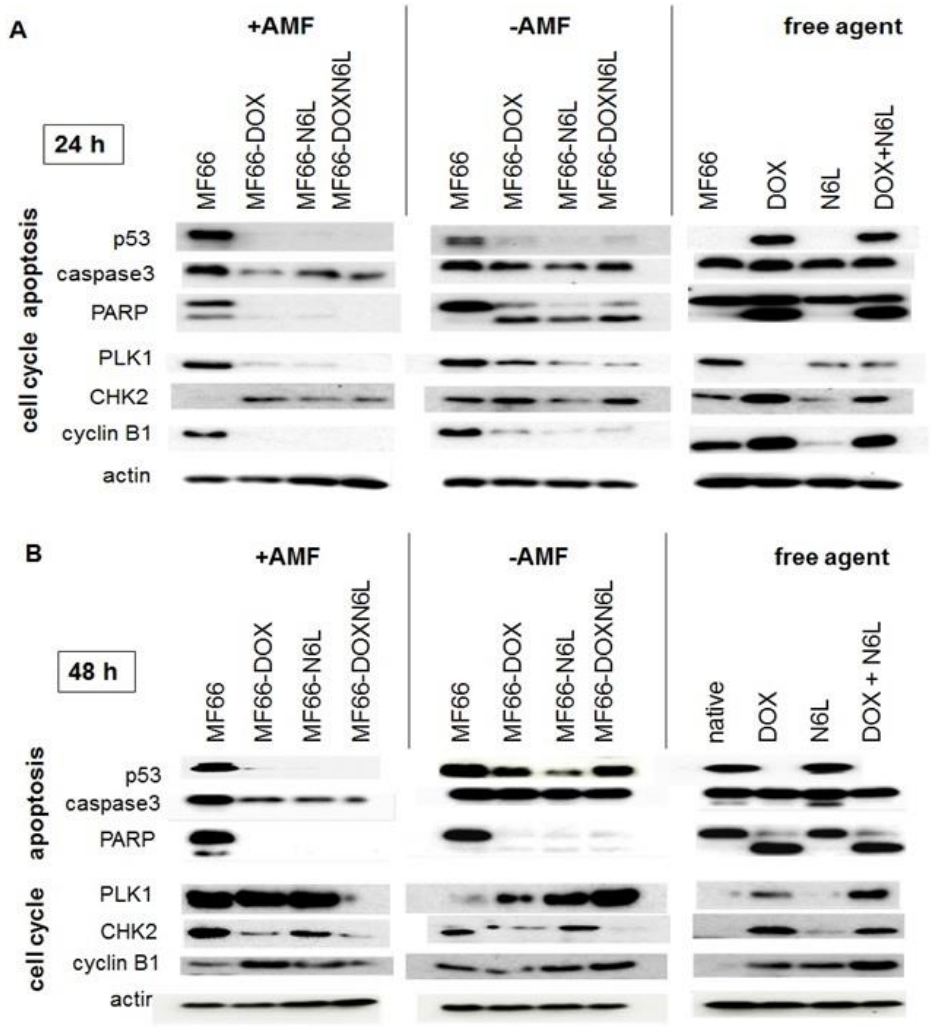

Figure 4. In vitro experiments confirmed that free DOX induced apoptosis and when functionalized to MNPs in combination with magnetic hyperthermia a G2/M checkpoint arrest in the BT474 cell line. BT474 cells were grown until confluence was reached and then incubated with 100 µg Fe/ml MNP or the free ligand (amount of free DOX comparable to concentration of DOX coupled to MNPs, 40 µmol DOX/ g iron) for 24 h and then exposed to an alternating magnetic field (AMF: H = 23.9 kA/m, f = 410 kHz, 60 min at 43 °C). 24 h (A) or 48 h (B) post hyperthermia, the cells were prepared for Western Blot analysis.

2.4 Combining DOX conjugated MNP with magnetic hyperthermia causes tumor regression in BT474 xenograft model. The presence of magnetic hyperthermia combined with DOX-functionalized or non-functionalized MNPs led to significant reduction of tumor volumes in mice compared to the untreated ones during the period of investigation (28 days)

Preprints (www.preprints.org) | NOT PEER-REVIEWED | Posted: 28 September 2018 doi:10.20944/preprints201809.0569.v1

(figure 5). Here, the relative tumor volumes decreased up to 50% compared to the initial volume measured at the beginning of the experiments (figure 5). In case of treating tumors with DOX conjugated MNPs the regression was obvious at six days post treatment whereas this effect was delayed (17 days post treatment) when non-functionalized MNPs were applied. Interestingly, the treatment of mice with DOX alone initially seemed to promote tumor growth up to day 10 and afterwards it dampened tumor growth, but the effect was not so prominent when conjugated to MNPs combined with magnetic hyperthermia (figure 5). The combined tumor therapy caused a regression of tumor growth in mice. Particularly in relation to DOX functionalized MNP, a high percentage of the tumor surface was covered with temperatures higher than 43 °C (suppl. figure 3).

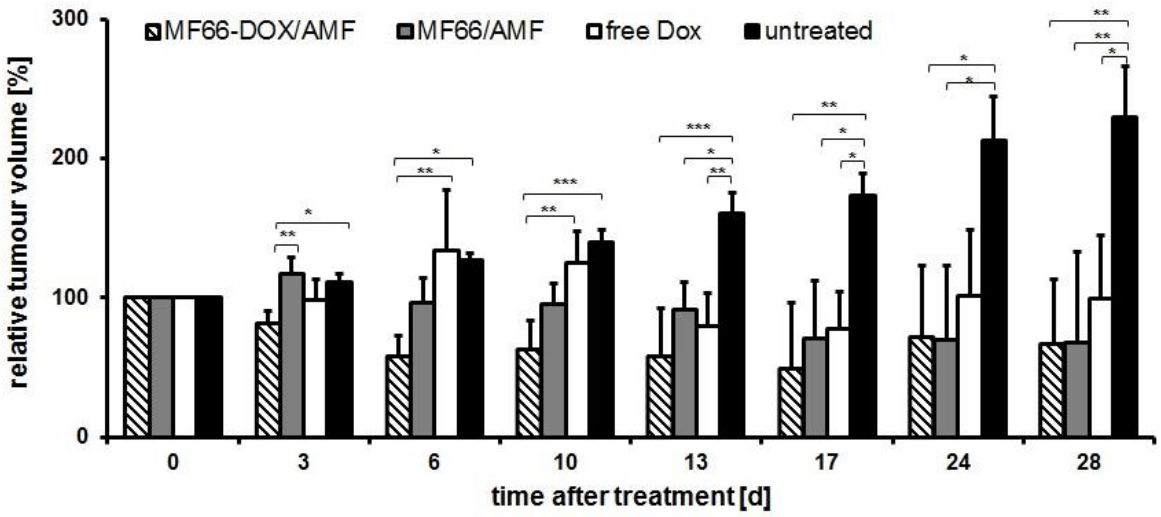

Figure 5. Combining MNP and magnetic hyperthermia significantly reduces tumor volumes *in vivo*. Relative tumor volumes to day 0, in %, mean ± SD (n ≥ 4 mice per group).

2.5 Magnetic hyperthermia and the presence of DOX functionalized MNPs induce cell death and arrested cells in the G2/M phase of the cell cycle in vivo. 48 h after magnetic hyperthermia treatment, the presence of DOX in the MNP formulations led to an increase of pro-apoptodic marker p53, but not of caspase 3 and PARP, in the BT474 tumor bearing mice (figure 6). This contrasts with the effect of non-functionalized MNPs combined with hyperthermia and free DOX in the tumor bearing mice which accumulated the pro-apoptodic

Preprints (www.preprints.org) | NOT PEER-REVIEWED | Posted: 28 September 2018 doi:10.20944/preprints201809.0569.v1

proteins caspase 3 and PARP beside p53 (figure 6). With regard to the cell cycle, an increased expression of PLK1 as well as cyclin B1 was detectable in tumors of mice after combined treatment of DOX functionalized MNPs and magnetic hyperthermia, indicating an arrest in the G2/M phase of the BT474 cells (figure 6). Interestingly, during the intratumoral treatment of mice with non-functionalized MNPs in presence with magnetic hyperthermia and the antitumor agent DOX no effect on cyclin B1 expression was identifiable. With consideration of PLK1, we observed an enhanced expression within the tumor of mice (figure 6).

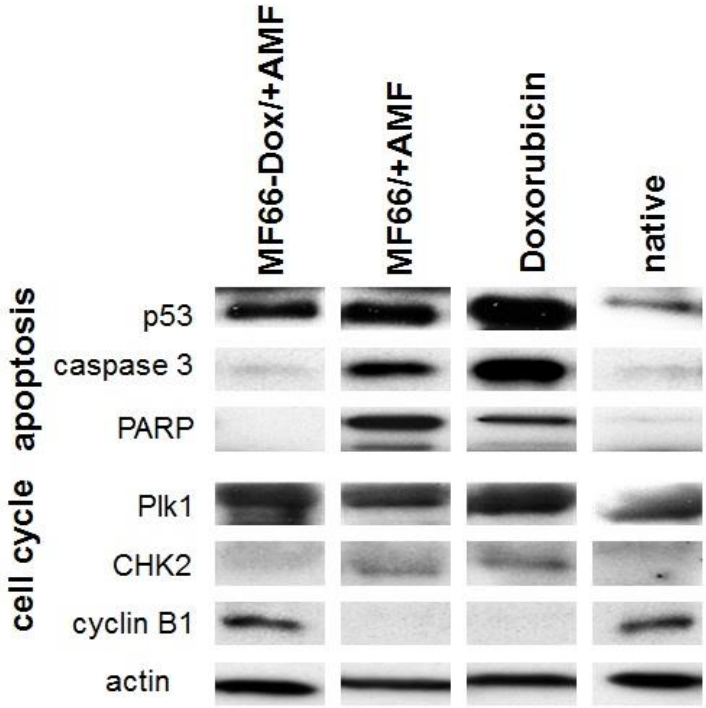

Figure 6. DOX functionalized MNPs combined with magnetic hyperthermia induced apoptosis and a G2/M checkpoint arrest in the BT474 cancer model *in vivo*. BT474 tumors were grown 28 days in mice, then MNP formulations or free DOX were applied intratumorally and exposed to an alternating magnetic field (AMF: H = 15.4 kA/m, f = 435 kHz, 60 min at 43 °C). 48 h post hyperthermia treatment tumors of mice were excised and the indicated proteins were analyzed via Western Blot.

2.6 The free antitumor agent DOX had a reversible effect on white blood cells and the administered functionalized and non-functionalized MNPs remain within the BT474-

Preprints (www.preprints.org) | NOT PEER-REVIEWED | Posted: 28 September 2018 doi:10.20944/preprints201809.0569.v1

tumor. With consideration of blood composition of tumor bearing mice, 14 days after treatment the white blood cells temporarily increase in presence of MNPs combined with magnetic hyperthermia (figure 7 A). By contrast, the free ligand DOX remarkably reduced the amount of white blood cells at this time point (figure 7 A). Both effects were compensated at a later time (28 days) to normal values. The number of red blood cells as well as the amount of haemoglobin did not alter after application of different treatment variants (figure 7 B, C).

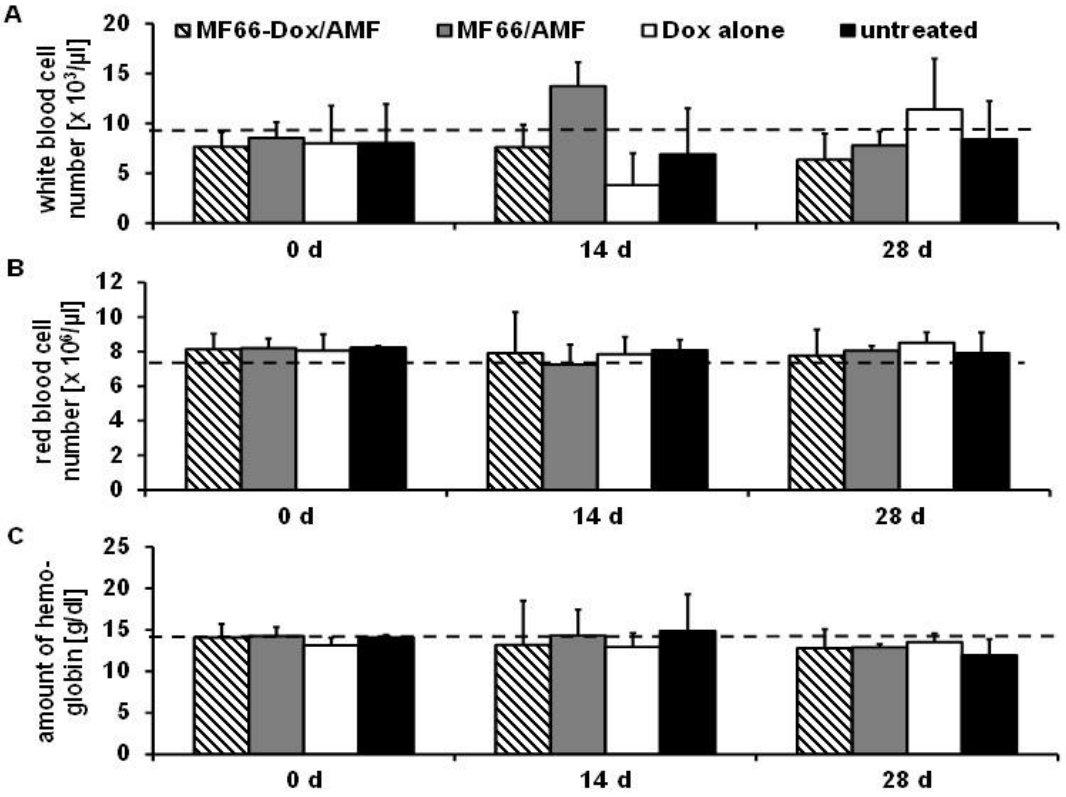

Figure 7. MNPs coupled with DOX are suitable for hyperthermia treatment indicated by the good biocompatibility. The blood composition of the animals was monitored over time after intratumoral MNP application. The number of white blood cells **(A)**, red blood cells **(B)**, and the amount of hemoglobin **(C)** are displayed for animals. Dashed lines refer to reference values (Harlan Laboratories, Venra, The Netherlands; http://www.harlan.com).

The intratumorally injected non-functionalized and DOX functionalized MNPs and the free ligand DOX exhibited different behaviour within the tumor (figure 8). Whereas the MNPs

Preprints (www.preprints.org) | NOT PEER-REVIEWED | Posted: 28 September 2018 doi:10.20944/preprints201809.0569.v1

formulations persisted within the tumor the free ligand DOX readily was removed from it (figure 8).

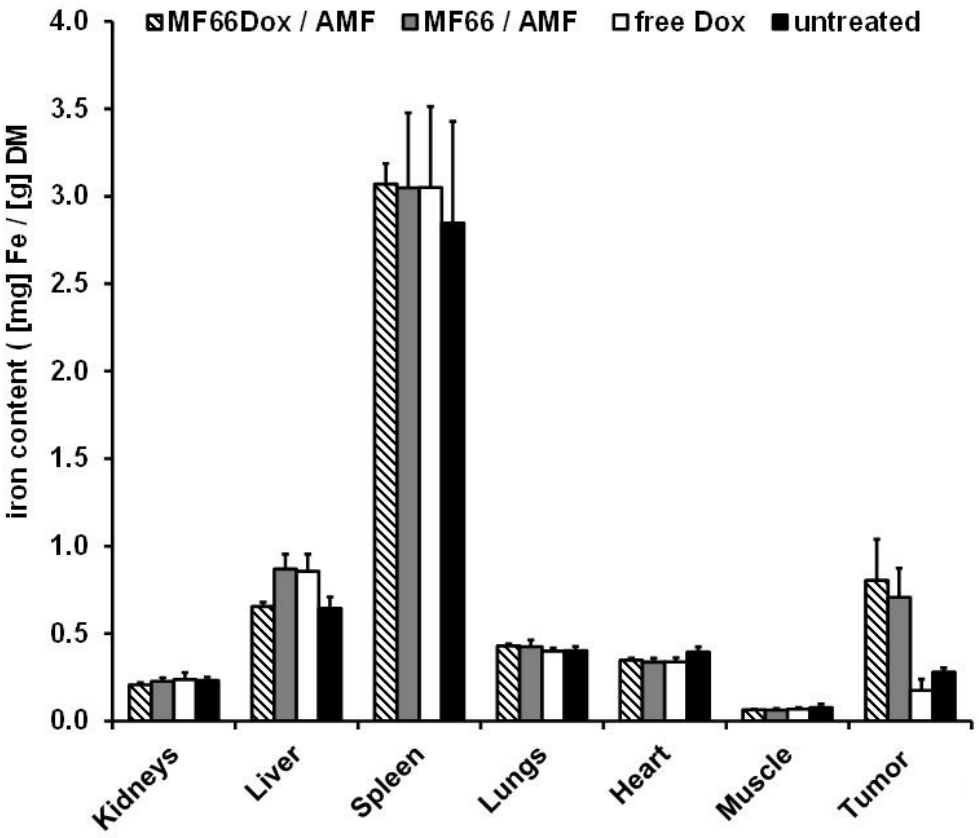

Figure 8. The intratumorally injected MNPs remain within the tumor after hyperthermia treatment. The spleen has a high intrinsic iron content even without MNP application. Means and SEM of n ≥ 4 animals/group.

3 Discussion

The results presented in this study clearly demonstrate a strengthened antitumor effect of DOX in breast cancer cells by functionalization of MNPs with the multivalent pseudopeptide N6L and DOX. We have shown that i) the presence of N6L on the surface of MNPs functionalized with DOX increases the internalization into a breast cancer cell line and potentiate the cytotoxic potential of the anticancer drug, ii) the treatment of a breast cancer cells with DOX functionalized MNPs combined with hyperthermia influences the expression of apoptotic

 doi:10.20944/preprints201809.0569.v1

proteins as well as proteins related to the cell cycle, iii) DOX functionalized MNPs in combination with hyperthermia favors tumor regression in vivo.

In particular, in water suspension the presence of DOX on MNPs alone did not lower ILP compared to non-functionalized MNPs, but the presence of N6L as well as both ligands DOX and N6L on MNPs distinctly lowered it. This is not due to clustering of MNP since PDI and zeta potential are almost similar. The reason could be an increase in size and corresponds to previously described features in the literature [22]. Nevertheless the bi-functionalized MNPs still showed good heating potential.

The results presented herein showed that the presence of N6L and more prominent the presence of DOX and N6L foster the uptake of MNPs into BT474 cells. Here, the pseudopeptide N6L binds to cell surface proteins nucleolin and nucleophosmin that are overexpressed in most tumor cells [20], [21]. Another possible mechanism by which N6L strengthened the internalization of MNPs includes the electrostatic interaction with sulfated glucosaminogylcans (GAGs) associated with cell surface [20], [23]. In this context the negatively charged sulfated GAGs interact with the positively charged N6L and this supports several studies indicating glucoaminoglycan-specific roles in cancer biology [24] [23]. Whereas the binding of N6L to tumor cells is partly due to tumor-specific cell surface target proteins, the uptake mechanism of DOX into the cells is more nonspecific. Basically there are two internalization mechanisms of DOX conjugated MNPs possible: a) DOX is released from MNPs outside the cell in the tumor environment and b) DOX enters the cell due to endocytosis of nanoparticles and is released inside the cell into acidic intracellular vesicles such as endosomes and lysosomes [25], [26]. In case of the DOX release outside the cell, the drug could interact with cell membranes by insertion into the lipid matrix [27], [28], [26]. Within membranes, anionic phospholipids were shown to be important targets for the hydrophobic agent [29]. Moreover passive diffusion is another mechanism of free DOX to enter the cell [29]. This mechanism is not specific and selective for cancer cells and presents a major disadvantage of conventional mode of DOX delivery. In case of the MNPs conjugated with both DOX and N6L, the internalization effects of each compound very likely to be additive

Preprints (www.preprints.org) | NOT PEER-REVIEWED | Posted: 28 September 2018 doi:10.20944/preprints201809.0569.v1

resulting in the best cellular uptake. In turn, the increased uptake of the MNPs functionalized with DOX and N6L is beneficial for therapeutic effects.

Moreover, we clearly demonstrate a reduced viability of target BT474 cells caused by DOX conjugated MNPs and this is potentiated when combined with magnetic hyperthermia and and N6L in a time-dependent manner in vitro. The increased uptake of MNPs conjugated with both DOX and N6L, as we discussed above, causes a higher presence of DOX within the tumor cell, likely accompanied by enhanced mechanism of actions, including oxidative damage and DNA double-strand breaks. Moreover the internalized MNPs into the tumor cells possibly contribute to the decreased cellular growth, too. The internalization of these MNPs through endocytosis and afterwards the exposure to an magnetic field generates intracellular heating spots resulting in an immediate destruction of cells [19], [30], [31], [22]. The effect was also seen via morphological changes of the cells. In absence of a magnetic field, the functionalized MNPs influence the viability of BT474 cells to a lesser extent. Based on these results we conclude that the reduced viability of BT474 cells is due to the combination of heating and the anticancer drug DOX. Both effects potentiate the cytotoxic effects on BT474 cancer cells.

The remarkable reduction of viability of BT474 cells after magnetic hyperthermia combined with MNPs conjugated with DOX alone and both DOX and N6L was not due to activation of p53, caspase-3 or PARP-1 in vitro, as we could demonstrated by Western Blot. Since all of the mentioned proteins play important roles in apoptotic pathways, mechanisms other than apoptosis lead to reduced cell viability [32], [33], [34], [35, 36]. Besides apoptosis there are several other mechanisms leading to programmed cell death, including autophagic cell death, paraptosis, pyroptosis, oncosis, programmed necrosis and caspase-independent cell death [35], [34]. Additionally, it is well conceivable that DOX is also acting due to such a autophagic pathway as shown for resveratrol, a type of polyphenol antioxidant that is found in various plants and fruits [37]. Interestingly, the free DOX (unbound form) activates apoptotic proteins in BT474 cells. But the effect on viability is less pronounced. One can conclude that observed overexpression of p53, PARP-1 and caspase 3 is associated rather with cell survival than with

Preprints (www.preprints.org) | NOT PEER-REVIEWED | Posted: 28 September 2018 doi:10.20944/preprints201809.0569.v1

apoptosis. There is evidence for contribution of the mentioned proteins in cellular survival [38], [39], [40].

Remarkably, the exposure of BT474 cells to DOX functionalized MNPs and hyperthermia indicated a distinct increase of polo-like kinase-1 (Plk-1) in contrast to the free agent or DOX coupled MNPs. Plk-1 belongs to the serine-threonine kinases and plays a critical role during mitotic progression and is involved in DNA damage checkpoint pathways [41], [42]. The level of Plk-1 expression fluctuates during cell cycle progression. The expression begins to increase in the S-phase and peaks at G2/M transition [41]. An overexpression of Plk-1 arrests BT474 cells in this phase might be well due to cellular repair processes. The repair process can be induced primary due to the treatment of cells with DOX and hyperthermia or as a secondary reaction to the treatment and selection of resistant cells. Moreover our data indicated that DOX conjugated MNPs combined with hyperthermia activated cyclin B1 most pronounced at later time points, in contrast to the free DOX, influencing cyclin B1 expression at rather time points. With regard of the effect of free agent DOX in the present study, a similar effect was shown for Adriamycin, an anthracycline antibiotic, in HeLa cells. A subcytotoxic concentration of Adriamycin transiently increased the expression level of cyclin B1 and afterwards decreased it, whereas the treatment with cytotoxic concentrations did not influence cyclin B1 expression [43]. Assuming a subcytotoxic field exists for DOX, it is conceivable that the used concentration of DOX in this study is within such a field and thus similar effects as for Adriamycin were caused in the cells. Furthermore it is known, that cyclin B1 is crucial for G2/M progression of the cell cycle [44]. Previous work figured out that treatment with DOX or topoisomerase inhibitors induced cyclin B1 accumulation, leading to G2/M phase arrest in a murine monocytic cell line and Jurkat cells [45], [46]. Moreover a substance similar to daunorubicin arrested Jurkat cells in the G2/M phase and induced DNA repair rather than cell death [47]. In accordance with the results of other working groups we conclude that the induction of cyclin B1 by DOX and DOX functionalized MNPs in the BT474 cells is related to induction of DNA repair responses rather than apoptosis. Indeed, the additional presence of N6L on DOX

Preprints (www.preprints.org) | NOT PEER-REVIEWED | Posted: 28 September 2018 doi:10.20944/preprints201809.0569.v1

conjugated MNPs combined with hyperthermia increased the uptake into the BT474 cells but seems not to further influence mechanisms investigated here.

Our in vivo experiments indicated a prominent reduction of tumor volumes particularly after treatment with DOX functionalized MNPs and hyperthermia. These effects were most pronounced between day 6 and 17 days after treatment. The effect of DOX and hyperthermia seemed to be additive during this time period. The additive effects combined metabolic effects of DOX, such as intercalation with DNA and causing DNA double-strand breaks, and of hyperthermia, including DNA stability, protein conformation and/or expression as well as production of reactive oxygen species [19], [1], [48], [49]. The results show that more than one therapy sessions (including the intratumoral application of MNP) might be necessary in order to achieve long-lasting anti-tumor effects on the tumor volume. One important reason is that due to irregularities in the intratumoral MNP distribution, at least in the used tumor model, in some cases regions of temperature underdosage might occur.

The in vivo effects of DOX conjugated MNPs combined with hyperthermia on protein expression were different from effects of mice treated with magnetic hyperthermia alone, even a comparable reduction of tumor volumes was identifiable. Whereas magnetic hyperthermia alone activated pro-apoptotic proteins, including p53, caspase 3 and PARP, the additional presence of DOX simply induces the expression of p53. We can conclude that the presence of DOX on the MNPs combined with hyperthermia changes the mechanism of action. But these mechanisms have to be studied in detail in the future. Moreover effects on expression of cell cycle proteins CHK2, cyclin B1 and Plk1 were comparable for DOX conjugated MNPs combined with hyperthermia in vivo and in vitro. In contrast DOX coupled MNPs combined with hyperthermia induced the expression of p53 in vivo, but not in vitro.

To sum up, the intratumoral application of DOX coupled MNPs might overcome biological barriers to chemotherapeutic drugs to penetrate into the target cells. In combination with hyperthermia these MNPs can be an effective method in enhancing the localised delivery and penetration of Doxorubicin into breast cancer cells.

4 Material and methods

Preprints (www.preprints.org) | NOT PEER-REVIEWED | Posted: 28 September 2018 doi:10.20944/preprints201809.0569.v1

4.1 Synthesis of magnetic nanoparticles (MNPs). Superparamagnetic iron oxide nanoparticles (MNPs), named MF66, were synthesized by co-precipitation technique as described previously [22]. They were coated with a dimercaptosuccnic acid (DMSA) and covalently conjugated either with the pseudopeptide Nucant (N6L; MF66-N6L; 4 µmol N6L/ g iron), the chemotherapeutic drug doxorubicin (DOX; MF66-DOX; 40 µmol DOX/ g iron) or both (MF66-N6LDOX; 40 µmol DOX/ g iron; 4µmol N6L/ g iron) as described previously [22]. The amount of immobilized N6L, DOX or both on the MF66-MNPs was quantified as described previously [22].

4.2 Characterization of MF66-MNPs. The core size of the non-functionalized and functionalized MNPs, the hydrodynamic diameter (expressed as Z-average size) and the Zeta potential (pH 7.4) of the MNPs were determined using Zetasizer equipment (Zetasizer Nano ZS, Malvern Instruments, Germany). To assess the heating potential of the different MF66 formulations the specific absorption rate (SAR) was determined in different environments (ferrofluid, immobilized in 10% polyvinyl alcohol and immobilized in cells 24 h after MNP incubation at 100 µg iron / ml) [50]. In order to compare SAR values with data in the literature the intrinsic loss power (ILP) was calculated as described elsewhere [50].

4.3 Cell culture. The BT474 cell line, a human breast invasive ductal carcinoma cell line, was selected because of their known sensitivity against magnetic hyperthermia and doxorubicin [51], [48]. BT474 cells were cultivated at 37°C in a humidified atmosphere containing 5% CO2 and maintained in DMEM with 10% (v/v) fetal bovine serum (FBS) supplemented with glutamax I, sodium pyruvate, glucose (4,5 g/l) (all products from Gibco®, Paisley, Scotland, UK). Cells were passaged after reaching up 90% of confluency. The workflow of the conducted the in vitro experiments with this cell line were shown in the supplements (suppl. figure 1).

4.4 Determination of cellular uptake of MNP formulations. Quantification of intracellular iron content 24 h after application of MNP formulations to BT474 cells was determined using flame atomic absorption spectrometry (AAS) as previously described [50].

Preprints (www.preprints.org) | NOT PEER-REVIEWED | Posted: 28 September 2018 doi:10.20944/preprints201809.0569.v1

4.5 *In vitro* magnetic hyperthermia. BT474 cells were incubated with non-functionalized (MF66), functionalized (MF66-DOX, MF66-N6L, MF66-N6LDOX) MNP in a concentration of 100 µg iron / ml or the equivalent molar amount of free ligands for 24 h at 37°C and 5% CO_2. Non-internalized MNPs as well as free agents were removed by washing steps. Cells without any additives were used to represent the normal metabolic state and referred to as native cells. Afterwards cells were exposed to an alternating magnetic field (AMF conditions: H = 23,9 kA / m, f = 410 kHz) and magnetically heated to a target temperature of 43°C for the duration of 1 h (+AMF group) or were placed in an incubator at 37°C for the same period of time (-AMF group). Temperature dose was monitored during AMF via fiber optic temperature sensor and thermometer.

4.6 Analysis of cell viability. Viability of BT474 cells was assessed 24 h or 48 h after magnetic hyperthermia treatment based on the dehydrogenase activity using AlamarBlue Cell Proliferation Reagent according to the manufacturer's instructions. Fluorescence was measured (Tecan Infinite M1000, excitation/emission: 530-560 nm / 590 nm). The relative dehydrogenase activity (rDH) was determined by normalizing the measured fluorescence of appropriate cells to the fluorescence of untreated cells.

4.7 Microscopy. To investigate the influence of magnetic hyperthermia on morphological changes and detachment of BT474 cells 24 h as well as 48 h after treatment light microscopy (Evos XL imaging system, Thermo Fisher Scientific) was used.

4.8 Prussian blue staining for iron detection in cells *in vitro*. Internalization and cellular uptake of MNPs (MF66, MF66-DOX 100 µg iron/ml, respectively) and free agent DOX (4 nmol/ml) in BT474 cells was determined as described previously [22].

4.9 Western Blot analysis. After magnetic hyperthermia treatment, BT474 cells were allowed to grow for additionally 24 h or 48 h in cell culture flasks before they were harvested, washed and lysed with RIPA lysis buffer containing protease inhibitors as described previously [52]. The following primary mouse antibodies against p53, caspase 3, cyclin B1, Plk-1 were

Preprints (www.preprints.org) | NOT PEER-REVIEWED | Posted: 28 September 2018 doi:10.20944/preprints201809.0569.v1

purchased from Santa Cruz biotechnology. Rabbit antibodies against PARP and phospho-CHK2 were obtained from Cell Signaling and mouse anti-actin was obtained from abcam. As secondary goat antibodies against mouse and rabbit IgG HRP were used from Santa Cruz biotechnology according to manufacturer's instructions. Chemoluminescence via horse radish peroxidase substrate was detected using a digital imaging system.

4.10 Murine xenograft model, tumor implantation and *in vivo* magnetic hyperthermia. All animal experiments were performed in accordance with international guidelines on the ethical use of animals and were approved by the regional animal care committee (Approval code 02-68/1,1 approval date 21th February 2012, Thüringer Landesamt für Verbraucherschutz, Bad Langensalza, Germany). Except tumor implantation all procedures are performed under inhalation anaesthesia using isoflurane in O_2 flow (2 %). Animals were humanely cared during the whole experimentation period. They were maintained under artificial day-night cycles and received food and water *ad libitum*. 3 days before subcutaneous BT474 cell pellet implantation, 17β-Estradiol pellet (0,36 mg, Innovative Research of America) was implanted subcutaneously in the region between shoulder and neck of female athymic nude mice (Hsd:Athymic Nude-Foxn1^{nu}, Harlan Laboratories, The Netherlands) to support in vivo BT474 cell growth. Afterwards 200 µl Matrigel containing 2x10^6 BT474 cells were injected subcutaneously on the rear backside of the mice and allowed tumor growth until a volume of 200 mm^3 was reached. Animals were divided into four independent treatment groups: Animals of Group 1 (therapy group) received an intratumoral injection of MF66Dox MNP (0.24 mg iron/100 mm^3 tumor volume; 40 µmol DOX/ g iron) and were exposed to an alternating magnetic field (H = 15.4 kA/ m; f = 435 kHz) for 1 h. Group 2 was used to investigate the impact of non-functionalized MF66 on tumor growth. In this context mice were injected intratumorally with MF66 MNP (0.24 mg iron/100 mm^3 tumor volume) and exposed to an alternating magnetic field at the same conditions as described above. Group 3 monitored the effect of free DOX (Doxorubicinhydrochlorid, cell pharm GmbH, Germany) whereby the animals received intratumorally DOX (9,6 nmol DOX/ 100 mm^3 tumor volume) but no hyperthermia treatment.

Preprints (www.preprints.org) | NOT PEER-REVIEWED | Posted: 28 September 2018 doi:10.20944/preprints201809.0569.v1

Group 4 was used to assess the normal tumor growth in absence of any treatment (intratumoral injection of aqua dest.).

4.11 In vivo effects of magnetic hyperthermia on tumor volume, temperature distribution in tumor tissue, blood count and protein expression. Tumor volume was monitored every three or four days as described elsewhere [52]. The assessment of temperature distribution within tumor area was determined as previously described [50]. Furthermore on day 1, 14 and 28 after the initial treatment, levels of red and white blood cells as well as amount of hemoglobin were determined via hematology (Sysmex pocH-100i, Sysmex GmbH, Germany). For analysis of protein expression pattern 48 h after treatment, Western blot analysis of excised and homogenized BT474 tumors was performed as described above. Subsequently, the lysates were prepared for Western Blot analysis with the use of the antibodies as mentioned above, except the antibody for caspase3, was purchased from Cell Signaling.

4.12 MNP distribution in vivo. At defined time points after treatment all mice were sacrificed and organs (kidneys, liver, spleen, lungs, heart), muscle tissue and tumors were extracted, dried and incinerated as described elsewhere [22]. Aliquots of each sample were measured using flame atomic absorption spectrometry (AAS).

4.13 Statistics. The level of significance was assessed by utilization of the Mann-Whitney-U-Test by comparison of treated samples or animals versus 37 °C treated samples or untreated animals. P values of ≤ 0.05 were chosen to be significantly different (*).

5 Supplementary Materials

Figure S1. Workflow of *in vitro* experiments with human breast adenocarcinoma BT474.

Figure S2. Cellular uptake of magnetic nanoparticles (MNPs) by BT474 cells *in vitro*. Internalization and uptake of MNPs (MF66, MF66-DOX, 100µg iron/ ml) in living BT474 cells was visualized 24 h or 48 h post-incubation in optical microscopy (blue spots) with Prussian blue reaction for iron oxide detection. Native BT474 cells or cells incubated with free DOX (the same concentration as coupled to the MNPs) did not show any blue staining. Scale bar 50 µm.

Preprints (www.preprints.org) | NOT PEER-REVIEWED | Posted: 28 September 2018 doi:10.20944/preprints201809.0569.v1

Figure S3. Temperature distribution maps (heat maps) of tumor surface temperatures of the two consecutive AMF treatments (first and second). The percentages of tumor area treated with temperatures below 43°C, between 43 and 45°C and above 45°C plotted against the individual relative tumor volume at 28 days after the first therapy are shown. BT-474 xenografts treated with magnetic hyperthermia using native (MF66) or functionalized (DOX) MNPs. *AMF* alternating magnetic field.

6 Acknowledgement

The described work was carried out within the project “Multifunctional Nanoparticles for the Selective Detection and Treatment of Cancer” (Multifun), funded by the European Commission (Nr. 262943) and the European Union’s Horizon 2020 research and innovation programme under grant agreement No 685795. IMDEA Nanociencia acknowledges support from the 'Severo Ochoa' Programme for Centres of Excellence in R&D (MINECO, Grant SEV-2016-0686). We thank Dr. Vijay Patel and Liquids Research Ltd (Mentec, Deiniol Road, Bangor, Gwynedd, North Wales, UK,) for the supply of MF66. We gratefully acknowledge Susann Burgold for technical assistance in carrying out in vivo experiments.

7 Author Contribution

Writing, original draft preparation- Susann Piehler; investigation and methology- Heidi Dähring , Julia Grandke, Julia Göring, Pierre Couleaud, Antonio Aires, Aitziber L. Cortajarena, José Courty, Alfonso Latorre, Álvaro Somoza; supervision and project administration- Rodolfo Miranda; review and editing- Álvaro Somoza, Ingrid Hilger; conceptualization, supervision, project administration- Ingrid Hilger

8 Conflicts of Interest

Ingrid Hilger declares that she is holding a patent DE 10 2005 062 746.

7 References

1. Ibrahim, M.K., et al., *Design, synthesis, molecular modeling and anti-proliferative evaluation of novel quinoxaline derivatives as potential DNA intercalators and topoisomerase II inhibitors.* Eur J Med Chem, 2018. **155**: p. 117-134.
2. de Oliveira Silva, J., et al., *Toxicological study of a new doxorubicin-loaded pH-sensitive liposome: A preclinical approach.* Toxicology and Applied Pharmacology, 2018. **352**: p. 162-169.
3. Swift, L.P., et al., *Doxorubicin-DNA adducts induce a non-topoisomerase II-mediated form of cell death.* Cancer Res, 2006. **66**(9): p. 4863-71.
4. Minotti, G., et al., *Anthracyclines: molecular advances and pharmacologic developments in antitumor activity and cardiotoxicity.* Pharmacol Rev, 2004. **56**(2): p. 185-229.
5. Gewirtz, D.A., *A critical evaluation of the mechanisms of action proposed for the antitumor effects of the anthracycline antibiotics adriamycin and daunorubicin.* Biochem Pharmacol, 1999. **57**(7): p. 727-41.
6. Huun, J., P.E. Lonning, and S. Knappskog, *Effects of concomitant inactivation of p53 and pRb on response to doxorubicin treatment in breast cancer cell lines.* Cell Death Discov, 2017. **3**: p. 17026.
7. Kim, H.S., Y.S. Lee, and D.K. Kim, *Doxorubicin exerts cytotoxic effects through cell cycle arrest and Fas-mediated cell death.* Pharmacology, 2009. **84**(5): p. 300-9.
8. Kabel, A.M., et al., *Targeting the proinflammatory cytokines, oxidative stress, apoptosis and TGF-beta1/STAT-3 signaling by irbesartan to ameliorate doxorubicin-induced hepatotoxicity.* J Infect Chemother, 2018.
9. Kratz, F., et al., *Acute and repeat-dose toxicity studies of the (6-maleimidocaproyl)hydrazone derivative of doxorubicin (DOXO-EMCH), an albumin-binding prodrug of the anticancer agent doxorubicin.* Hum Exp Toxicol, 2007. **26**(1): p. 19-35.
10. Bielack, S.S., et al., *Doxorubicin: Effect of different schedules on toxicity and anti-tumor efficacy.* European Journal of Cancer and Clinical Oncology, 1989. **25**(5): p. 873-882.
11. Hu, J., et al., *Design of tumor-homing and pH-responsive polypeptide-doxorubicin nanoparticles with enhanced anticancer efficacy and reduced side effects.* Chem Commun (Camb), 2015. **51**(57): p. 11405-8.
12. Taratula, O., et al., *Multifunctional nanomedicine platform for concurrent delivery of chemotherapeutic drugs and mild hyperthermia to ovarian cancer cells.* Int J Pharm, 2013. **458**(1): p. 169-80.
13. Nigam, S. and D. Bahadur, *Doxorubicin-loaded dendritic-Fe3O4 supramolecular nanoparticles for magnetic drug targeting and tumor regression in spheroid murine melanoma model.* Nanomedicine, 2018. **14**(3): p. 759-768.
14. Babincova, N., et al., *Applications of magnetoliposomes with encapsulated doxorubicin for integrated chemotherapy and hyperthermia of rat C6 glioma.* Z Naturforsch C, 2018.
15. Pan, C., et al., *Theranostic pH-sensitive nanoparticles for highly efficient targeted delivery of doxorubicin for breast tumor treatment.* Int J Nanomedicine, 2018. **13**: p. 1119-1137.
16. Fojtu, M., et al., *Reduction of Doxorubicin-Induced Cardiotoxicity Using Nanocarriers: A Review.* Curr Drug Metab, 2017. **18**(3): p. 237-263.
17. Thirunavukkarasu, G.K., et al., *Magnetic field-inducible drug-eluting nanoparticles for image-guided thermo-chemotherapy.* Biomaterials, 2018. **180**: p. 240-252.
18. Islamian, J.P., M. Hatamian, and M.R. Rashidi, *Nanoparticles promise new methods to boost oncology outcomes in breast cancer.* Asian Pac J Cancer Prev, 2015. **16**(5): p. 1683-6.
19. Ludwig, R., et al., *Nanoparticle-based hyperthermia distinctly impacts production of ROS, expression of Ki-67, TOP2A, and TPX2, and induction of apoptosis in pancreatic cancer.* Int J Nanomedicine, 2017. **12**: p. 1009-18.
20. Destouches, D., et al., *Multivalent pseudopeptides targeting cell surface nucleoproteins inhibit cancer cell invasion through tissue inhibitor of metalloproteinases 3 (TIMP-3) release.* J Biol Chem, 2012. **287**(52): p. 43685-93.

21. Destouches, D., et al., *A Simple Approach to Cancer Therapy Afforded by Multivalent Pseudopeptides That Target Cell-Surface Nucleoproteins.* Cancer Research, 2011. **71**(9): p. 3296-3305.
22. Kossatz, S., et al., *Efficient treatment of breast cancer xenografts with multifunctionalized iron oxide nanoparticles combining magnetic hyperthermia and anti-cancer drug delivery.* Breast Cancer Res, 2015. **17**: p. 66.
23. Sader M, P.C., Gilles Carpentier, Maud-Emmanuelle Gilles, Noureddine Bousserrhine, Alexandre Livet, Ilaria Cascone, Damien Destouches, Aitziber L Cortajarena and José Courty, *Functionalization of Iron Oxide Magnetic Nanoparticles with the Multivalent Pseudopeptide N6l for Breast Tumor Targeting.* Journal of Nanomedicine & Nanotechnology, 2015. **06**(04).
24. Bracci, L., et al., *The GAG-specific branched peptide NT4 reduces angiogenesis and invasiveness of tumor cells.* PLoS One, 2018. **13**(3): p. e0194744.
25. Unsoy, G., et al., *Synthesis of Doxorubicin loaded magnetic chitosan nanoparticles for pH responsive targeted drug delivery.* Eur J Pharm Sci, 2014. **62**: p. 243-50.
26. Wong, H.L., et al., *A new polymer-lipid hybrid nanoparticle system increases cytotoxicity of doxorubicin against multidrug-resistant human breast cancer cells.* Pharm Res, 2006. **23**(7): p. 1574-85.
27. Cui, P.F., et al., *A new strategy for hydrophobic drug delivery using a hydrophilic polymer equipped with stacking units.* Chem Commun (Camb), 2018. **54**(59): p. 8218-8221.
28. Parker, M.A., V. King, and K.P. Howard, *Nuclear magnetic resonance study of doxorubicin binding to cardiolipin containing magnetically oriented phospholipid bilayers.* Biochim Biophys Acta, 2001. **1514**(2): p. 206-16.
29. Speelmans, G., et al., *Verapamil competes with doxorubicin for binding to anionic phospholipids resulting in increased internal concentrations and rates of passive transport of doxorubicin.* Biochim Biophys Acta, 1995. **1238**(2): p. 137-46.
30. Mailander, V. and K. Landfester, *Interaction of nanoparticles with cells.* Biomacromolecules, 2009. **10**(9): p. 2379-400.
31. Kim, J.S., et al., *Cellular uptake of magnetic nanoparticle is mediated through energy-dependent endocytosis in A549 cells.* J Vet Sci, 2006. **7**(4): p. 321-6.
32. Mendoza-Rodriguez, C.A. and M.A. Cerbon, *[Tumor suppressor gene p53: mechanisms of action in cell proliferation and death].* Rev Invest Clin, 2001. **53**(3): p. 266-73.
33. Sharpless, N.E. and R.A. DePinho, *p53: good cop/bad cop.* Cell, 2002. **110**(1): p. 9-12.
34. Bouchard, V.J., M. Rouleau, and G.G. Poirier, *PARP-1, a determinant of cell survival in response to DNA damage.* Exp Hematol, 2003. **31**(6): p. 446-54.
35. Savitskaya, M.A. and G.E. Onishchenko, *Mechanisms of Apoptosis.* Biochemistry (Mosc), 2015. **80**(11): p. 1393-405.
36. Morris, G., et al., *Cell Death Pathways: a Novel Therapeutic Approach for Neuroscientists.* Mol Neurobiol, 2018. **55**(7): p. 5767-5786.
37. Scarlatti, F., et al., *Role of non-canonical Beclin 1-independent autophagy in cell death induced by resveratrol in human breast cancer cells.* Cell Death And Differentiation, 2008. **15**: p. 1318.
38. Mirzayans, R., et al., *The Growing Complexity of Cancer Cell Response to DNA-Damaging Agents: Caspase 3 Mediates Cell Death or Survival?* Int J Mol Sci, 2016. **17**(5).
39. Elkholi, R. and J.E. Chipuk, *How do I kill thee? Let me count the ways: p53 regulates PARP-1 dependent necrosis.* Bioessays, 2014. **36**(1): p. 46-51.
40. Zhang, D., et al., *The interplay between DNA repair and autophagy in cancer therapy.* Cancer Biol Ther, 2015. **16**(7): p. 1005-13.
41. Kumar, S., et al., *PLK-1: Angel or devil for cell cycle progression.* Biochim Biophys Acta, 2016. **1865**(2): p. 190-203.
42. Jang, Y.J., et al., *Regulation of Polo-like kinase 1 by DNA damage in mitosis. Inhibition of mitotic PLK-1 by protein phosphatase 2A.* J Biol Chem, 2007. **282**(4): p. 2473-82.

43. Kikuchi, I., et al., *A decrease in cyclin B1 levels leads to polyploidization in DNA damage-induced senescence.* Cell Biol Int, 2010. **34**(6): p. 645-53.
44. Zuryn, A., et al., *Expression of cyclin A, B1 and D1 after induction of cell cycle arrest in the Jurkat cell line exposed to doxorubicin.* Cell Biol Int, 2012. **36**(12): p. 1129-35.
45. Ling, Y.H., et al., *Cell cycle-dependent cytotoxicity, G2/M phase arrest, and disruption of p34cdc2/cyclin B1 activity induced by doxorubicin in synchronized P388 cells.* Mol Pharmacol, 1996. **49**(5): p. 832-41.
46. Aytac, U., et al., *Effect of CD26/dipeptidyl peptidase IV on Jurkat sensitivity to G2/M arrest induced by topoisomerase II inhibitors.* Br J Cancer, 2003. **88**(3): p. 455-62.
47. Villamarin, S., et al., *Induction of G(2)/M arrest and inhibition of c-myc and p53 transcription by WP631 in Jurkat T lymphocytes.* Biochem Pharmacol, 2002. **63**(7): p. 1251-8.
48. Bandekar, A., et al., *Antitumor efficacy following the intracellular and interstitial release of liposomal doxorubicin.* Biomaterials, 2012. **33**(17): p. 4345-52.
49. Kampinga, H.H. and E. Dikomey, *Hyperthermic radiosensitization: mode of action and clinical relevance.* Int J Radiat Biol, 2001. **77**(4): p. 399-408.
50. Kossatz, S., et al., *High therapeutic efficiency of magnetic hyperthermia in xenograft models achieved with moderate temperature dosages in the tumor area.* Pharm Res, 2014. **31**(12): p. 3274-88.
51. Friedrich, R.P., et al., *Flow cytometry for intracellular SPION quantification: specificity and sensitivity in comparison with spectroscopic methods.* Int J Nanomedicine, 2015. **10**: p. 4185-201.
52. Stapf, M., U. Teichgraber, and I. Hilger, *Methotrexate-coupled nanoparticles and magnetic nanochemothermia for the relapse-free treatment of T24 bladder tumors.* Int J Nanomedicine, 2017. **12**: p. 2793-2811.